УДК 577. 323

THEORETICAL INVESTIGATION OF INTERACTION OF LOW-ENERGY PROTONS WITH CARBON AND FLUORINATED CARBON NANOSTRUCTURES

P.V. Avramov, B.I. Yakobson
and G.E. Scuseria*

We have performed a comparative study of the interaction process of low-energy protons (2-7 eV) with carbon (CNS) and fluorinated carbon nanostructures (FCNS) using molecular dynamics and ab-initio *Unrestricted Hartri-Fock 6-31G* and semiempirical PM3 methods. It has been shown that starting with a distance of 6 E from the CNS a charge transfer process transforms a proton and a CNS into hydrogen atom and positive ion-radical and leads to creation of a new C-H bond outside the carbon cage. The fluorination of CNS suppresses the charge transfer process, and proton interacts with FCNS as a point charge with neutral molecule. It leads to reduction of the penetration barriers by 2-4 times. At the same time the barrier for the escape of H^+ out of the FCNS remains high.*

I. INTRODUCTION

An endohedral carbon nanostructures are expected to have important future applications in the areas of magnetism, superconductivity, treatment of cancer, energy production and storage, etc. At present there are only few methods to synthesize such fascinating structures: (i) High-temperature synthesis of fullerenes and nanotubes with some chemical substances [1, 2], (ii) synthesis under high pressure (H_2, He) [3, 4], (iii) using high-energy ion beams [5] and (iiii) penetration of some atoms inside the carbon cage as a result of radioactive decay [6]. Only for ion beams in the case of Li^+ [7] the chemical yield reaches 30%, in all other cases the yield is equal to 0.1 ÷ 0.01% or less. Formation of endohedral and exohedral complexes with metal ions frequently leads to dramatic changes in chemical properties of the carbon cages [8] due to transformation of the cages to the ion-radicals and creation of a set of polymer structures.

Previously the potential barriers of the proton penetration inside the fullerene cage [9] have been studied at *ab initio* PRDDO and DFT levels of theory. The barrier has been calculated as a difference between the energy of the ground state of $C_{60}H$ (H covalently bounded outside the cage with one of the carbon atom, the system has neutral charge) and the energy of a neutral transition complex with the proton in the center of the relaxed six member ring. It has been shown that the potential barrier is equal to 3.8 eV. The potential barrier of the penetration of He atom inside the fullerene cage was calculated by molecular mechanics [10] (9.4 eV), semiempirical MNDO [11] (11.5 eV) and post Hartre-Fock MP2/6-31G** [12] (10.7 eV for C_6H_6) methods. The MD simulation of Li^+ ion penetration inside the fullerene cage [13] has been performed on DFT level of theory. It has been shown that the barrier of the penetration is less than 5 eV.

A creation of an efficient way of synthesis of hollow carbon nanostructure endohedral complexes is an important goal of modern chemistry. The immediate cause of high penetration barriers and low chemical yield of the existent schemes is a rich p-electron system of carbon nanostructures, that favors of the creation of new covalent bonds on the outer surface of the objects. The reasonable way to eliminate the system is saturation of double C-C bonds by fluorine. At present the most fluorinated derivative of C_{60} molecule is $C_{60}F_{48}$ [14].

II. ELECTRONIC STRUCTURE OF HIGLY FLUORINATED FULLERENES AND COMPUTATIONAL MODELS

The $C_{60}F_{48}$ molecule (Fig. 1) has S_6 symmetry group [14]. There are 3 types of carbon hexagons: with 6 fluorine atoms (2 pieces), with 5 fluorine atoms (12 pieces) and with 4 fluorine atoms (6 pieces) and 2 types of pentagons with 5 fluorine atoms (6 pieces) and with 3 fluorine atoms (6 pieces). There are 6 double C-C bonds (1.31 E) (*ab initio* 6-31G* results) and 3 types of single C-C bonds (1.49, 1.54, 1.56 1.59 E). The length of C-F single bond is equal to 1.34 E. The electronic structure of highly fluorinated $C_{60}F_{48}$ [14] was studied by photoelectron spectroscopy and by *ab initio* RHF/6-31G [15] method.

In this work we study an interaction of low energy protons (2-7 eV) with CNS (C_6H_6 and C_{60}) and FCNS (C_6F_{12} and $C_{60}F_{48}$). To understand the role of p-electron system we study the potential barriers of He atom penetration into pristine and fluorinated carbon nanostructures. The atomic and electronic structures of a number of C_6H_6, C_6F_{12}, C_{60} and $C_{60}F_{48}$ structures with protons and helium atoms in different positions have been calculated by the *Gaussian* suite of programs [16] using *ab initio* UHF/6-31G* method and semiempirical UHF PM3 method. The geometry optimization has been carried out using analytic energy gradient. All potential barriers have been calculated with taking into account Basis Set

---

© * P.V. Avramov, Department of Chemistry of Krasnoyarsk State University, Krasnoyarsk, Russia; B.I. Yakobson, L.V. Kirensky Institute of Physics SB RAS, Krasnoyarsk, Russia; G.E. Scuseria, Department of Chemistry and Center for Biological and Environmental Nanotechnology, Rice University, Houston, Texas 77005-1892, 2003.

Superposition Error (BSSE). The process of penetration of low energy protons inside the carbon cages has been simulated by molecular dynamics using UHF PM3 (MD/PM3) and *ab initio* UHF/6-31G* (MD/6-31G*) potentials.

The initial state of the irradiation process is unsteady: there is a proton on infinity and neutral molecule as a target (Fig. 1). Due to the big energy difference (Table 1) between the ionization potentials of CNS (as C_{60} etc.) and hydrogen atom, a charge transfer process should occur at a reasonable distance between the proton and the CNS. Using the first order perturbation theory we can write (a proton moves along Z-direction):

$$H = H_0^H + H_0^{CN} + V(R_{CN}) - \frac{\nabla_p^2 (R_{CN})}{2m_p} \tag{1}$$

where H_0^H and H_0^{CN} are Hamiltonians of unperturbed hydrogen atom and CNS/FCNS, a perturbation operator $V(R_{CN}) = V^H(R_H) + V^{CN}(R_{CN}) = -\frac{q_C}{|r_H - R_C|} + \frac{q_F}{|r_H - R_F|} - \frac{1}{|r_{CN} - R_H|}$ describes a proton – CNS/FCNS interactions, q_C, q_F are Mulliken atomic charges of carbon (q_C=0 in the case of C_{60} and ~0.1 in the case of $C_{60}F_{48}$) and fluorine (q_F~-0.1 in the case of $C_{60}F_{48}$). $R_{CN} = \sqrt{\frac{2E_K^p}{m_p}}t$ is a proton-CNS/FCNS distance, R_{CN} is measured between the proton and the center of a carbon hexagon (fully fluorinated in the case of C60F48), t varies from $-\infty$ to 0, $-\frac{\nabla_p^2 (R_{CN})}{2m_p}$ is an operator of kinetic energy of a proton, E_K^p is kinetic energy of a proton (~10 eV in our case). Modern molecular dynamics [18] is eligible for singularities on the potential surfaces close to the Born-Openheimer (BO) ones. Taking into account $m_p/m_e \cong 2*10^3$ ratio and averaged kinetic energy of valence electrons ($E_K^e \sim 10eV$) the BO approximation is appropriate for the MD simulations of the irradiation processes up to $E_K^p \sim 10^2 \div 10^3 eV$.

In that case we can separate the electron and nuclear parts of the Eq. 1. In the first order of perturbation theory for the electronic part of the Eq. 1 we can write:

$$\varepsilon'_H = \varepsilon_H^0 + \Delta\varepsilon_H \tag{2}$$

$$\varepsilon'_{CN} = \varepsilon_{CN}^0 + \Delta\varepsilon_{CN} \tag{3}$$

$\varepsilon_H^0 = -13.6eV$, for C_{60} $\varepsilon_{CN}^0 = -7.6eV$ and for the $C_{60}F_{48}$ $\varepsilon_{CN}^0 = -12.3eV$ (experimental values [17] and [14], Table 1). Eigenvalues $\varepsilon'_H(R_H)$ and $\varepsilon'_{CN}(R_{CN})$ describe new energies derived from the ε_H^0 and ε_{CN}^0.

A probability of electron transition between the perturbed $\varphi'_{CN}(r_{CN})$ and $\varphi'_H(r_H)$ states, derived from unperturbed C2p_z and H1s, can be expressed [19] in the form:

$$w_T = 2|L_T|^2 / (\hbar\omega)^2 \tag{4}$$

where $L_T = \langle \varphi'_{CN}(r_{CN}) | r(R_{CN}) | \varphi'_H(r_H) \rangle$, r($R_{CN}$) is an operator of dipole electron transitions, energy of transition $\hbar\omega = \varepsilon'_{CN}(R_{CN}) - \varepsilon'_H(R_{CN})$. The matrix elements $L_T \neq 0$ when overlapping integrals $S_{H-CN} = \langle \varphi'_H | \varphi'_{CN} \rangle \neq 0$. At large distances R_{CN} (Fig.1) the overlapping integrals are equal to 0. Our ab initio UHF/6-31G* calculations show that

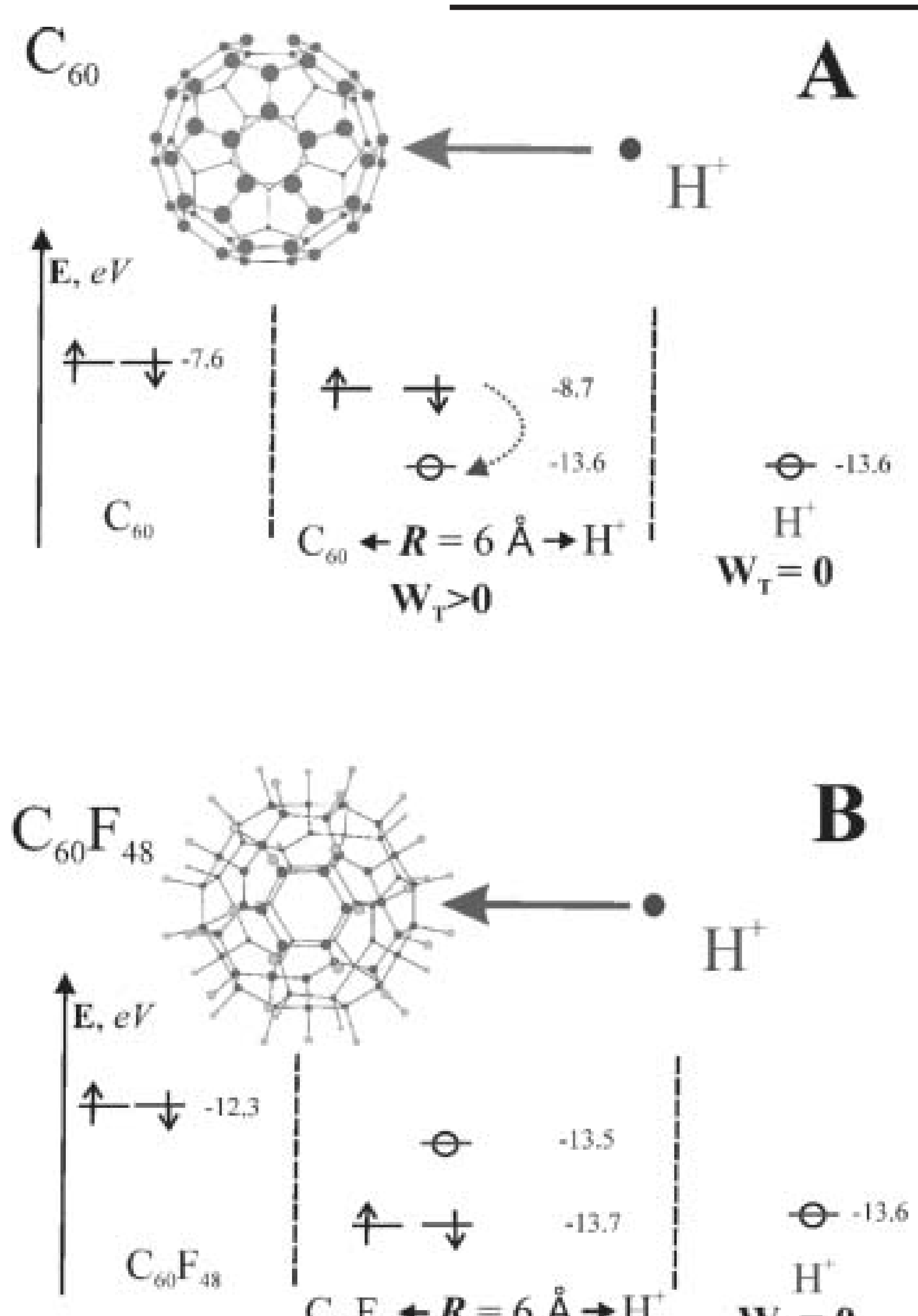

Fig. 1. Chart of the proton beam irradiation process for C_{60} (A) and $C_{60}F_{48}$ (B) cases. On the right side the unperturbed eigenvalue ε_{H}^{0} (in read) of hydrogen is presented. On the left side the unperturbed eigenvalue ε_{CN}^{0} of CNS/FCNS (in black) is presented. In the middle perturbed $\varepsilon_{CN}^{'}$ and $\varepsilon_{H}^{'}$ eigenvalues derived from ε_{CN}^{0} and ε_{H}^{0} are presented. W_T is a probability of electronic charge transfer transition at different distances from carbon nanostructure to proton. At the distances of $0 \div 6$ E for the C_{60} case W_T varies from 0 to 1. For the C_{60} case the transition converts an exited configuration with fully occupied unperturbed $\varphi_{CN}^{0}(r_{CN})$ and vacant $\varphi_{H}^{0}(r_{H})$ states into ground state configuration with partially occupied $\varphi_{CN}^{'}(r_{CN})$ and occupied $\varphi_{H}^{'}(r_{H})$ states. For the $C_{60}F_{48}$ case the electronic charge transfer transition does not realized due to $\varepsilon_{CN}^{'} < \varepsilon_{H}^{'}$ condition.

Table 1

Theoretical and experimental ionization potentials of H, C_{60} and $C_{60}F_{48}$

Object	UHF PM3 (eV)	*ab initio* UHF 6-31G* (eV)	Experiment (eV)
H	13.1	13.6	13.6
C_{60}	9.5	7.6	7.6 [17]
$C_{60}F_{48}$	14.2	13.8	12.3 [14]

overlapping integrals change from 0 to 0.5 at distances of 6 ÷ 0 E from the center of a six member carbon ring ($R_C < 6.3$ E, $R_F < 5.8$ E). For that interval $r(R_{CN})$ is equal to several E, so $w_T \approx S_{H\text{-}CN}$. At the distance of 6 E for the $C_{60}F_{48}$ (PM3 results) $\Delta\varepsilon_H = 0.1eV$ and $\Delta\varepsilon_{CN} = -1.4eV$ $\left(\varepsilon'_H = -13.5, \varepsilon'_{CN} = -13.7eV\right)$. So, at distances ≤6 E the configuration $C_{60}F_{48}$+proton becomes the ground state of the system and FCNS should interacts with the proton as neutral molecule with a point charge (Fig. 1).

For the C_{60} $\Delta\varepsilon_H = 0.0eV$ (Mulliken charge of carbon atoms are equal to 0) and $\Delta\varepsilon_{CN} = -1.15eV$ $\left(\varepsilon'_H = -13.6eV, \varepsilon'_{CN} = -8.7eV\right)$. The frequency ω is equal to 10^{16} s^{-1}, so $w_T \approx 1$ (4). A low energy proton (~2 eV) overcomes the distance of 6 E in the $T=5*10^{-14}$ sec. (the number of periods of electronic transition from the occupied $\varphi'_{CN}(r_{CN})$ state (Fig.1) into vacant $\varphi'_H(r_H)$ state for the system C_{60}+proton at the distance <6 E is proportional to $10^2 \div 10^3$). Based on the values of experimental width of electronic transitions from the photoelectron spectra (0.2 ÷ 0.3 eV) of C_{60} [20, 21] and $C_{60}F_{48}$ [14] we can estimate the life time of the exited electronic state $\tau \sim 5*10^{-15} \div 3*10^{-15}$, which is big enough for the transition of the system into ground state (neutral hydrogen atom + C_{60}^{+1} ion-radical).

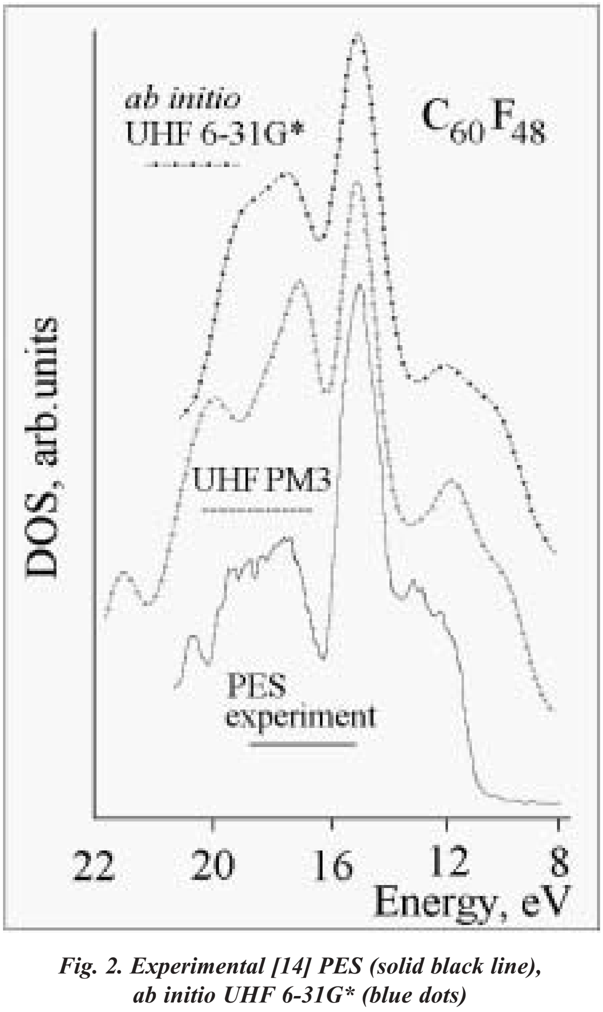

Fig. 2. Experimental [14] PES (solid black line), ab initio UHF 6-31G (blue dots) and PM3 UHF (pink triangles) DOS of $C_{60}F_{48}$*

Both theoretical methods used in the work correctly describe the initial state of the FCNS+proton system due to overestimation of the first ionization potential of the $C_{60}F_{48}$ (Table 1). This feature allows us to use MD/PM3 and MD/6-31G* methods to simulate collisions of protons with FCNS (C_6F_{12} and $C_{60}F_{48}$) under different kinetic energies. For a comparison we performed the same *ab initio* MD simulations for C_{60} and C_6H_6 with one exception: to avoid of the incorrect description of the initial electronic state (proton on infinity and a neutral carbon nanostructure as a target) the starting distance between the proton and the center of a carbon hexagon was equal to 2 E. For the C_6H_6, and C_6F_{12} we used both UHF PM3 and *ab initio* UHF 6-31G* potentials and for C_{60} and $C_{60}F_{48}$ only UHF PM3 one.

To test the adequacy of PM3 method for MD simulations we compared density of electronic states (DOS) (Fig. 2) obtained with UHF PM3 and *ab initio* UHF/6-31G* methods with experimental DOS obtained by photoelectron spectroscopy [14]. Fig. 2 demonstrates the quantitative agreement of theoretical DOSes obtained by UHF PM3 and *ab initio* UHF/6-31G* with experimental one.

III. RESULTS AND DISCUSSION

To study the process of penetration of a proton into the carbon cages we calculated the potential energy curves for interaction of the proton with C_{60} (Fig. 3b) and $C_{60}F_{48}$ (Fig. 3a) using UHF PM3 and *ab initio* UHF/6-31G* methods. The distance R_{CN} is measured between the proton and the center of a carbon hexagon (fully fluorinated in the case of $C_{60}F_{48}$). Black solid lines are *ab initio* UHF 6-31G* potential curves, blue dots are UHF PM3 potential curves. Black (*ab initio* UHF 6-31G*) and blue (UHF M3) triangles at distances

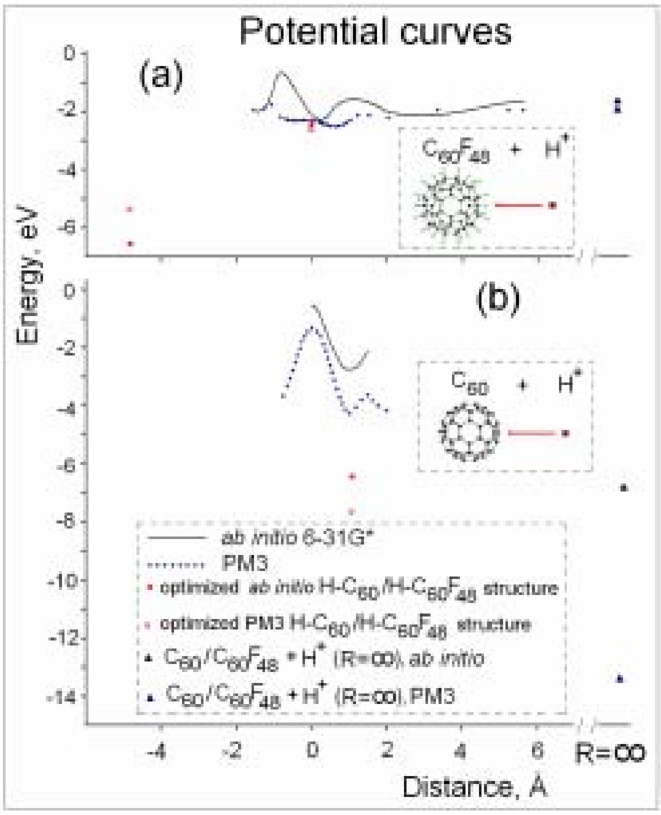

Fig. 3. Potential curves of $C_{60}F_{48}$ + H^+ (a) and C_{60} +H^+ interactions (b). Black solid lines are ab initio UHF 6-31G* potential curves, blue dots are UHF PM3 potential curves. Black (ab initio UHF 6-31G*) and blue (UHF M3) triangles at distances R= ∞ indicate total energies of $C_{60}F_{48}$ (a) and C_{60} molecules. Solid (ab initio UHF 6-31G*) and empty (UHF PM3) red circles indicate total energies of optimized H-$C_{60}F_{48}^+$ (a) (in the center of hexagon ring (R=0 E) and covalently bounded inside the carbon cage (R=-5 E)) and H-C_{60}^+ (b) (covalently bounded outside the carbon cage (R=1 E)) structures

R= ∞ indicate total energies of $C_{60}F_{48}$ and C_{60} molecules. Solid (*ab initio* UHF 6-31G*) and empty (UHF PM3) red circles indicate total energies of optimized H-$C_{60}F_{48}^+$ (a) (in the center of hexagon ring (R=0 E) and covalently bounded with *sp*^{2} carbon inside the carbon cage (R=-5 E)) and H-C_{60}^+ (b) (covalently bounded with *sp*^{2} carbon outside the carbon cage (R=1 E)) structures.

The potential curves demonstrate smooth behavior for the $C_{60}F_{48}$ + H^+ process without big potential barriers outside the carbon wall and in the center of the fully fluorinated hexagon. A deep potential hole exists inside the carbon (R=-5 E) nanocage due to covalent bonding of a proton with *sp*^{2} carbon atom. The C_{60} + H^+ process demonstrates a different behavior of the potential curves along *z*-direction: There is a big energy minimum at infinity (neutral C_{60} molecule) and outside the carbon cage (R=1 E, covalently bonded hydrogen). It is necessary to note that the last energy minimum does not belong to the *z*-direction and reflects ordinary C-H *sp*^{3} covalent bond.

The potential barriers of proton penetration have been calculated as a energy difference between the transition state of the process (guest atom in the center of the hexagon carbon ring) and the initial state (the proton coordinated to a carbon atom on the equilibrium C-H distance outside the cage [9] *or as energy difference between the transition state and free C_{60} molecule). For the penetration of He atom the initial state is C_{60}/$C_{60}F_{48}$ molecule + He on infinity. A kinetic energy of penetration has been calculated by the MD simulations as a minimal kinetic energy which is necessary to proton to penetrate through the carbon hexagon. In the case of $C_{60}F_{48}$ we performed the MD simulations trough the fully fluorinated carbon hexagons. The results are presented in Table 2 (*ab initio* UHF 6-31G*) and Table 3 (UHF PM3).

The *ab initio* UHF/6-31G* calculations (Table 2) have demonstrated a great reduction (up to 4 times in the case of C_6H_6 and C_6F_{12}) of the potential barrier for H^+ penetration through the fluorinated carbon nanostructures (C_6F_{12} and $C_{60}F_{48}$) in comparison with the pristine C_{60} and C_6H_6 molecules. We explain the result by the existence of active p electron system on the top of the valence band of the CNS. The elimination or decreasing the π-density prevents a creation of the new C-H bond outside the carbon cage in the process of proton interaction with a FCNS. On the other hand (see Fig. 3) a potential barrier for escape of a proton from the carbon cage remains high (~5 eV, Fig. 3) due to creation of a new C-H covalent bond inside the cage.

The potential barrier for He atom is 25% lower in the case of the $C_{60}F_{48}$ in comparison with C_{60} (Table 2). The interatomic C-C distance in $C_{60}F_{48}$ (1.59E) is 12.5% larger than the same distance (1.40E) for the C_{60} molecule, so the decreasing of the barrier can not be explained only by the increasing of the hexagon diagonal for the FCNS and can be induced by the elimination of the p-electron density in the center of the hexagon. That fact also clearly demonstrates an importance of the chemical interaction of a proton with the carbon wall in the process of penetration.

We performed the MD/6-31G* simulations for C_6H_6 and C_6F_{12} molecules. Kinetic energy of a proton for penetration through the C_6 fragment is 2.6 times lower for C_6F_{12} molecule (2.6 eV) in comparison with the C_6H_6 (6.7 eV) (Table 2). We

Table 2

Potential barriers and kinetic energies of proton for penetration through the carbon hexagon ring. *Ab initio* 6-31G* UHF results.

Object	Potential barrier, eV	Kinetic energy, eV
C_6H_6+H^+	5.6	6.7
C_6F_{12}+H^+	1.4	2.6
C_{60}+H^+	6.2 (6.3*)	-
$C_{60}F_{48}$+H^+	3.1	-
C_{60}+He	14.0	-
$C_{60}F_{48}$+He	10.5	-

*Potential barrier has been calculated as energy difference between the transition state (proton in the center of the carbon hexagon) and C_{60} molecule. BSSE error has been taken into account.

Table 3

Potential barriers and kinetic energies of proton for penetration through the carbon hexagon ring. PM3 UHF results

Object	Potential barrier, eV	Kinetic energy, eV
C_6H_6+H^+	6.5	5.6
C_6F_{12}+H^+	4.8	3.7
C_{60}+H^+	6.5 (12.0*)	5.7
$C_{60}F_{48}$+H^+	1.8	1.4

*Potential barrier has been calculated as energy difference between the transition state (proton in the center of the carbon hexagon) and C_{60} molecule.

did not study a potential surface for the C_6F_{12}+H^+ system due to sufficient deformation of the C_6 fragment in the molecule.

The similar results have been obtained by semiempirical PM3 method (Table 3). The potential barrier (1.8 eV) for the $C_{60}F_{48}$ is 3.6 times lower than in the case of C_{60} (6.5 eV). The same ration for the pair C_6F_{12} (4.8 eV) and C_6H_6 (6.5 eV) is much lower (~1.4) due to the fact that PM3 method predicts a breaking of C-C bond in C_6F_{12} molecule by H^+. The MD/PM3 simulations gave the same ratios of the kinetic energy of a proton for C_{60}/$C_{60}F_{48}$ (4.1) and C_6H_6/C_6F_{12} (1.5). It is necessary to note that after the penetration through the carbon wall of the $C_{60}F_{48}$ a proton creates new C-H covalent bond with a sp^2 carbon atom inside the cage. The next steps of protonation can create either a new C-H bond or a H_2 molecule by destroying previously created C-H bond.

We studied other channels of inelastic scattering of a proton on $C_{60}F_{48}$ by MD/PM3 simulations. To perform the study we choose the next targets for a proton:

1) a carbon atom not covered by fluorine
2) center of double C-C bond
3) center of a pentagon
4) a fluorine atom
5) center of C-F bond
6) off-center position of a hexagon
7) off-center position of a pentagon.

It has been shown by MD/PM3 simulations that there are some inelastic scattering channels of a proton with energy higher the 1.8 eV:

1. Breaking of C-F bond (collisions with a carbon atom, with center of C-C double bond, with center of C-F bond).
2. Penetration into the carbon cage (collisions with the center of pentagon ring and partially off-center collisions with hexagon rings).
3. Reflection with partial dissipation of the proton kinetic energy due to creation of molecular oscillations of $C_{60}F_{48}$ (off-center collisions with pentagon and hexagon rings, collisions with F atoms).

Using the MD/PM3 simulations it has been shown that a hole with 1.5E diameter exists in the center of all hexagon rings for penetration of a proton with a kinetic energy ~1.8 eV. It means that approximately 25% of surface of $C_{60}F_{48}$ is accessible for penetration of low energy protons.

VI. CONCLUSIONS

It has been shown that charge transfer process plays the main role in proton-CNS interaction at distance smaller than 6 E. Due to the process the low energy protons turn into hydrogen atoms and interact with pristine carbon nanostructures as radicals with ion-radicals with creation new covalent C-H bonds outside the carbon cage. Fluorination of the carbon cage suppresses the charge transfer process and the low energy protons interact with the FCNS as point charges with neutral molecules. Based on the *ab initio* UHF/6-31G* and UHF PM3 calculations, MD/6-31G* and MD/PM3 simulations it has been shown that fluorination of hollow carbon nanostructures can decrease the penetration barrier for H^+ by 2-4 times. Up to 25% of the surface of carbon cage can be accessible for low energy proton penetration. On the other hand the potential barrier for escape remains high due to the formation of a new covalent C-H bond inside the carbon cage. Other channels of inelastic scattering can lead to the breaking of the C-F chemical bond. The elimination of the p-system can decrease the penetration barrier for He atom up to 25%.

REFERECES

1. Heath J.R. et al. // J.Am.Chem.Soc. 1985, 107, 7779;
2. Chai Y. et al. // J.Phys.Chem. 1991, 95, 7564;
3. Sanders M. et al. // Science 1993, 259, 1428;
4. Christian J.J., Wan Z., Anderson S.L. // Chem. Phys. Lett. 1992, 199, 373;
5. Murphy T.A. et al. // Phys. Rev. Lett. 1996, 77, 1075;
6. Ohtsuki T. et al. // Phys. Rev. Lett. 1998, 81, 967;
7. Campbell E.E.B. et al. // J. Phys. Chem. Solids 1997, 58 1763;
8. Bethune D.S. et al. // Z. Phys. D 1993, 26, 153;
9. Estreicher S.K., Lathan C.D., Heiggie M.I., Jones R., Цberg S. // Chem. Phys. Lett. 1992, 196, 311;
10. Mowrey K.C., Ross M.M., Callahan J.H., J. Phys. Chem. 1992, 96, 4755;
11. Kolb M., Thiel W., J. Comp. Chem. 1993, 14, 37;
12. Hrusak J., Bцhme D.K., Weiske T., Schwarz H. // Chem. Phys. Lett. 1992, 193, 97;
13. Ohno K., Maruyama Y., Esfarjani K., Kawazoe Y. // Phys. Rev. Lett. 1996, 76, 3590;
14. Mitsumoto R. et al. // J. Phys. Chem. A 1998, 102, 552;
15. Bulusheva L.G., Okotrub A.V., Boltalina O. V. // J. Phys. Chem. A 1999, 103, 9921;
16. Frisch M. J., Trucks G. W., Schlegel H. B. et al. // GAUSSIAN 01, Development Version (Revision B.01), Gaussian Inc., 2001Pittsburgh, PA;
17. Hedberg K., Hedberg L., Bethune D.S., Brown C.A., Dorn H.C. // Science 1991, 254, 410;
18. Car R., Parinello M. // Phys. Rev. Lett. 1985, 55, 22, 2471;
19. Landau L.D., Lifshic E.M. // Quantum mechanics, nonrelativistic theory, Nauka 1974, Moscow;
20. Weaver J.H. // Acc. Chem. Res. 1992, 25, 143;
21. Varganov S.A., Avramov P.V., Ovchinnikov S.G. // Physics of the Solid State 2000, 42, 2103;

ТЕОРЕТИЧЕСКОЕ ИССЛЕДОВАНИЕ ВЗАИМОДЕЙСТВИЯ НИЗКОЭНЕРГЕТИЧЕСКИХ ПРОТОНОВ С УГЛЕРОДНЫМИ И ФТОРУГЛЕРОДНЫМИ НАНОСТРУКТУРАМИ

П.В. Аврамов, Б.И. Якобсон, Г.Е. Скусерия

В работе проведено сравнительное моделирование процесса взаимодействия низкоэнергетических протонов с углеродными и фторуглеродными наноструктурами методами квантовой химии и молекулярной динамики. Было показано, что начиная с расстояния 6 Е от углеродной стенки процесс зарядового переноса превращает протон в атом углерода, а углеродную наноструктуру – в положительный ион-радикал, что приводит к образованию ковалентной связи углерод-водород с внешней стороны углеродной стенки. Фторирование углеродных наноструктур приводит к подавлению процесса зарядового переноса, и низкоэнергетические протоны взаимодействуют с фторуглеродными наноструктурами как точеные заряды с нейтральными молекулами. Это, в свою очередь, приводит к уменьшению барьеров проникновения протона внутрь фторуглеродных структур в 2-4 раза по сравнению с немодифицированными углеродными структурами. С другой стороны, барьер выхода протона из углеродной сферы остается высоким в любом случае.